Beamforming Optimization for STAR-RIS-Assisted Integrated Sensing and Communication

1st Fangce Zhao
School of Information and Electronics
Beijing Institute of Technology
Beijing, China
1120221185@bit.edu.cn

2nd Zhenglun Pan
School of Information and Electronics
Beijing Institute of Technology
Beijing, China
1120223124@bit.edu.cn

3rd Xiyue Xia
School of Information and Electronics
Beijing Institute of Technology
Beijing, China
1120231165@bit.edu.cn

4th Minghao Yuan
School of Information and Electronics
Beijing Institute of Technology
Beijing, China
minghaoyuan@bit.edu.cn

5th Dongxuan He
School of Information and Electronics
Beijing Institute of Technology
Beijing, China
dongxuan_he@bit.edu.cn

6th Huazhou Hou
Pervasive Communication Research Centre
Purple Mountain Laboratories
Nanjing, China
houhuazhou@pmlabs.com.cn

2025 International Wireless Communications and Mobile Computing (IWCMC) | 979-8-3315-0887-6/25/$31.00 ©2025 IEEE | DOI: 10.1109/IWCMC65282.2025.11059504

***Abstract*—In this paper, simultaneously transmitting and reflecting reconfigurable intelligent surface (STAR-RIS)-assisted integrated sensing and communication (ISAC) is considered. Based on constraints of communication signal-to-interference-plus-noise ratio (SINR), maximum transmit power limitation, and the law of conservation of energy, the objective is to maximize the SINR of the radar perception signal. To address this non-convex maximization problem, a novel method rooted in fractional programming (FP) and block coordinate descent (BCD) is introduced. To handle non-convex constraints, an alternative optimization algorithm grounded in BCD is introduced. To tackle the non-convex problem of fractional form, the original formulation is optimized utilizing fractional programming techniques, thereby transforming it into a convex problem for more efficient solution. Additionally, select conditions are relaxed through the application of semidefinite relaxation (SDR) techniques. Finally, the numerical results show that: 1) As the number of iterations increases, the proposed algorithm shows good convergence. 2) The performance of the proposed algorithm is significantly better than the state-of-the-art algorithms.**

***Index Terms*—Simultaneous transmitting and reflecting reconfigurable intelligent surface (STAR-RIS), integrated sensing and communication (ISAC), beamforming, fractional programming (FP), block coordinate descent (BCD), semidefinite relaxation (SDR).**

I. Introduction

The exploration of sixth-generation (6G) technology is accelerated all over the world. 6G will not only enhance communication speed and coverage, but also explore new frequency bands and more intelligent application scenarios [1]. Moreover, there is a growing recognition that future communication systems must not only possess robust communication capabilities but also exhibit enhanced intelligent sensing functionality [2]. In this context, the concept of integrated sensing and communication (ISAC) has been introduced, aimed at facilitating collaborative efforts between sensing and communication functions through the allocation of hardware and software resources [3].

Currently, the study of ISAC mainly focuses on dual-function radar and communication [4], [5] and the coexistence system of communication and radar [6], [7]. According to [8], [9], multi-antenna technology stands as a pivotal characteristic within ISAC to ensure the diversity of waveforms where the spatial degrees of freedom (DoF) are fully harnessed. Nevertheless, the significant path loss and obstructed paths for transmission result in signal degradation and a sudden drop in performance. To address this issue, the concept of reconfigurable intelligent surfaces (RIS) has been introduced. In particular, RIS consisting of multiple reflective elements can establish a virtual line of sight (LoS) when there is no practical link and also aligns these signals precisely with users or targets. The authors in [2], [10], [11], and [12] investigated the integration of RIS within ISAC systems. The authors in [2] and [10] emphasized system performance metrics, notably the radar signal-to-noise ratio (SNR), while simultaneously considering constraints such as quality of service (QoS). Conversely, [11] and [12] focused on the capability of RIS in aiding user localization. However, numerous prior studies have primarily focused on scenarios that the BS, users, and targets are all positioned on the same side of the RIS, thereby significantly limiting their practical applicability.

Motivated by the aforementioned works, we consider a more pragmatic model known as simultaneous transmitting and reflecting reconfigurable intelligent surface (STAR-RIS). STAR-RIS, as a variant of RIS, not only retains the capacity to reflect signals and alter their phase, but also possesses the unique ability to permit signals to traverse through it, thereby enabling BS, users, and targets to be situated on different sides of the STAR-RIS. In particular, the major contributions of our paper are as follows: 1) A STAR-RIS-assisted ISAC model containing multiple users and one target is proposed, where radar signal-to-interference-plus-noise ratio (SINR) maximization is the optimization goal. 2) fractional programming (FP)-block coordinate descent (BCD) based optimization algorithm

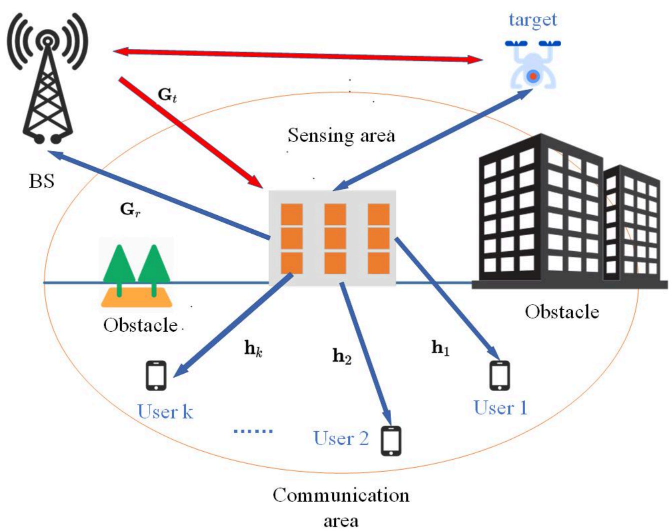

Fig. 1. Illustration of the considered STAR-RIS-assisted ISAC system.

is proposed, which can split the problem into several sub problems and transform the complex parts into simple forms.

$Notations$: Scalars, vectors, and matrices are denoted by lower-case letters, bold-face lower-case letters, and bold-face upper-case letters, respectively. $\mathbb{C}^{N\times M}$ and $\mathbb{R}^{N\times M}$ represents the space of $N \times M$ complex matrices and real matrices, respectively. $\mathbf{a}^*$ denotes the conjugate of vector $\mathbf{a}$; $\mathbf{a}^H$ denotes the conjugate transpose of vector $\mathbf{a}$; $diag(\mathbf{a})$ represents a diagonal matrix whose main diagonal elements are the elements of $\mathbf{a}$. $\mathbb{E}\{\cdot\}$ represents the mathematical expectation. $exp\{\cdot\}$ denotes the natural exponential function. $\mathrm{tr}(\mathbf{A})$ and $\mathrm{rank}(\mathbf{A})$ denote the trace and rank of matrix $\mathbf{A}$. $\mathbf{I}_K$ represents a K-order identity matrix. $\mathcal{CN}(\mu, \sigma^2)$ denotes a normal distribution with mean equal to μ and variance equal to σ^2.

II. System Model

Consider a STAR-RIS-assisted ISAC system consisting of a base station (BS), K single-antenna users, and a sensing target. In this system, the BS is equipped with a uniform linear array (ULA) with M transmit antennas and N_r receive antennas, while the STAR-RIS is equipped with a uniform planar array (UPA) consisting of N elements. As shown in Fig.1, the entire space is partitioned by STAR-RIS into two distinct parts, namely, the sensing area and the communication area. The target is located within the sensing area, while the users are located within the communication area. Moreover, we assume that the sensing area is located on the reflective side of the STAR-RIS, while the communication area is on the transmissive side of the STAR-RIS. Additionally, we consider that there exists a direct link from the BS to the target, but the direct links from the BS to the users are blocked by obstacles.

A. Signal Model And STAR-RIS Model

To achieve sensing and communication functionalities simultaneously, the signal transmitted by the BS needs to contain both communication signals and sensing signals, given by

$$\mathbf{s} = \mathbf{W}\mathbf{s}_c + \mathbf{s}_r, \tag{1}$$

where $\mathbf{s}_c \in \mathbb{C}^{K\times 1}$ represents the communication signal transmitted to K users satisfying $\mathbf{s}_c \sim \mathcal{CN}(0, \mathbf{I}_K)$, $\mathbf{W} = \{\mathbf{w}_1, \mathbf{w}_2, ..., \mathbf{w}_K\} \in \mathbb{C}^{M\times K}$ represents the communication beamformer, $\mathbf{s}_r \in \mathbb{C}^{M\times 1}$ denotes the radar signal for target sensing satisfying $\mathbb{E}\left\{\mathbf{s}_r\mathbf{s}_r^H\right\} = \mathbf{R}_r$ and $\mathbb{E}\left\{\mathbf{s}_c\mathbf{s}_r^H\right\} = \mathbf{0}$. Therefore, the covariance matrix of the transmitted signal can be expressed as

$$\mathbf{R}_s = \mathbb{E}\left\{\mathbf{s}\mathbf{s}^H\right\} = \mathbf{W}\mathbf{W}^H + \mathbf{R}_r. \tag{2}$$

In addition, STAR-RIS divides the signal into transmitted signals and reflected signal, to communication area and sensing area, respectively, thus requiring STAR-RIS to have two phase-shifting matrices. Denote $\mathbf{\Theta}_r \in \mathbb{C}^{N\times N}$ as refection phase-shifting matrices, and $\mathbf{\Theta}_t \in \mathbb{C}^{N\times N}$ as transmission phase-shifting matrices. The two phase-shifting matrices can be expressed as

$$\mathbf{\Theta}_i = \mathrm{diag}\left(\beta_{i,1}e^{j\varphi_{i,1}}, ..., \beta_{i,N}e^{j\varphi_{i,N}}\right), i \in \{t, r\}, \tag{3}$$

where $\beta_{i,n} \in [0, 1]$ and $\varphi_{i,n} \in [0, 2\pi]$ represent the amplitude and phase responses of the n-th element of STAR-RIS, respectively. Due to the law of energy conservation, the reflection phase-shifting matrix and the transmission phase-shifting matrix should satisfy

$$\beta_{t,n}^2 + \beta_{r,n}^2 = 1, \forall n \in \mathcal{N}. \tag{4}$$

However, due to signal loss caused by transmission loss and STAR-RIS imperfection, the sum of the total energy of the transmitted signal and the reflected signal may be much less than the signal received by STAR. Therefore, (4) can be rewritten as

$$\beta_{t,n}^2 + \beta_{r,n}^2 \leq 1, \forall n \in \mathcal{N}. \tag{5}$$

B. Communication Model

Assume that the channel state information (CSI) is known, we define $\mathbf{G}_t \in \mathbb{C}^{N\times M}$ as complex baseband channel between the BS and the STAR-RIS, $\mathbf{h}_k \in \mathbb{C}^{N\times 1}$ as complex baseband channel between the STAR-RIS and the k-th user. Therefore, the signal received by the k-th user can be expressed as

$$y_k = \mathbf{h}_k^H\mathbf{\Theta}_t\mathbf{G}_t\mathbf{s} + n_k, \tag{6}$$

where $n_k \sim \mathcal{CN}\left(0, \sigma^2\right)$ denotes the additive white Gaussian noise (AWGN) at k-th user with the variance σ^2. To evaluate the communication performance in such a multi-user system, the SINR is selected as the performance metric, where the SINR received by the k-th user can be calculated as

$$\gamma_k = \frac{\left|\mathbf{h}_k^H\mathbf{\Theta}_t\mathbf{G}_t\mathbf{w}_k\right|^2}{\sum_{i\in K\setminus k}\left|\mathbf{h}_k^H\mathbf{\Theta}_t\mathbf{G}_t\mathbf{w}_i\right|^2 + \mathbf{h}_k^H\mathbf{\Theta}_t\mathbf{G}_t\mathbf{R}_r\mathbf{G}_t^H\mathbf{\Theta}_t^H\mathbf{h}_k + \sigma^2}. \tag{7}$$

To guarantee effective communication, the SINR for each communication user should exceed a certain threshold, i.e., $\gamma_k \geq \bar{\gamma}_k$.

C. Sensing Model

The transmission steering vector of the BS can be expressed as

$$\mathbf{a}_t(\theta_h, \theta_v) = \exp\left(-j\left[\mathbf{x}, \mathbf{y}, \mathbf{z}\right]\mathbf{k}(\theta_h, \theta_v)\right), \tag{8}$$

while the reflection steering vector of the BS can be expressed as

$$\mathbf{a}_r(\theta_h, \theta_v) = \exp\left(-j\left[\bar{\mathbf{x}}, \bar{\mathbf{y}}, \bar{\mathbf{z}}\right]\mathbf{k}(\theta_h, \theta_v)\right), \tag{9}$$

where $[\mathbf{x}, \mathbf{y}, \mathbf{z}] \in \mathbb{R}^{M\times 3}$ denotes the Cartesian coordinates of transmit antennas of the BS, and $[\bar{\mathbf{x}}, \bar{\mathbf{y}}, \bar{\mathbf{z}}] \in \mathbb{R}^{M\times 3}$ denotes the Cartesian coordinates of receive antennas of the BS. We assume that the azimuth direction-of-arrival (DOA) θ_h and elevation DOA θ_v are unknown. $\mathbf{k}(\theta_h, \theta_v) \in \mathbb{R}^{3\times 1}$ represents the waveform vector as

$$\mathbf{k}(\theta_h, \theta_v) = \frac{2\pi}{\lambda}\left[\cos\theta_h\cos\theta_v, \sin\theta_h\cos\theta_v, \sin\theta_v\right]^T, \tag{10}$$

where λ denotes the wavelength of the carrier signal. Without loss of generality, the transmit antenna and the receive antenna of the BS are assumed to be located along the x-axis, which means $\mathbf{y} = \mathbf{z} = \bar{\mathbf{y}} = \bar{\mathbf{z}} = 0$. The BS and the target are assumed to be at the same elevation, which means $\theta_v = 0$. Therefore, the steering vector can be simplified as

$$\mathbf{a}_t(\theta_h) = \exp\left(-j\frac{2\pi}{\lambda}\mathbf{x}\cos\theta_h\right), \tag{11}$$

$$\mathbf{a}_r(\theta_h) = \exp\left(-j\frac{2\pi}{\lambda}\bar{\mathbf{x}}\cos\theta_h\right). \tag{12}$$

There are a total of four paths for the radar signals transmitted by the base station to reach the target and then be reflected back, namely BS - target - BS channel, BS - STAR-RIS - target - BS channel, BS - target - STAR-RIS - BS channel, BS - STAR-RIS - target - STAR-RIS - BS channel, respectively. As shown in [13], due to the severe fading of three-hop and four-hop transmissions, the signals received by the BS through BS - STAR-RIS - target - BS channel, BS - target - STAR-RIS - BS channel, BS - STAR-RIS - target - STAR-RIS - BS channel are very weak and can be neglected. Therefore, the radar echo signals received by the BS can be expressed as

$$\mathbf{y}_r = \alpha\mathbf{a}_r(\theta_h)\mathbf{a}_t^H(\theta_h)\mathbf{s} + \mathbf{G}_r\boldsymbol{\Theta}_r\mathbf{G}_t\mathbf{s} + \mathbf{n}_r, \tag{13}$$

where α represents the reflection coefficient of the target determined by the radar-cross section (RCS) of the target and the path loss, $\mathbf{G}_r \in \mathbb{C}^{N_r\times N}$ denotes the complex baseband channel between the STAR-RIS and the BS, and $\mathbf{n}_r \sim \mathcal{CN}(0, \sigma^2\mathbf{I}_{N_r})$ denotes the AWGN at the BS. Since communication signals can also be used for sensing and carrying target information, they are not considered as interference terms. In contrast, the signals reflected back are regarded as interference terms. Thus, the radar SINR can be expressed as

$$\gamma_r = \frac{\mathrm{tr}\left(\mathbf{A}\mathbf{R}_s\mathbf{A}^H\right)}{\mathrm{tr}\left(\mathbf{B}\mathbf{R}_s\mathbf{B}^H\right) + \sigma^2}, \tag{14}$$

where $\mathbf{A} = \alpha\mathbf{a}_r(\theta_h)\mathbf{a}_t^H(\theta_h)$, $\mathbf{B} = \mathbf{G}_r\boldsymbol{\Theta}_r\mathbf{G}_t$.

III. FP-BCD Based Optimization Design

In this section, we consider the beamforming optimization for STAR-RIS enabled ISAC.

A. Problem Formulation

Our primary objective is to maximize the radar SINR γ_r while ensuring that a SINR threshold γ_k can be satisfied for each communication user. To tackle this intricate non-convex optimization problem, we initially transform it into a more tractable form with the help of fractional programming.

The maximization of user SINR is equivalent to solving the following optimization problem, given by

$$\max_{\chi} \quad \frac{\mathrm{tr}\left(\mathbf{A}\mathbf{R}_s\mathbf{A}^H\right)}{\mathrm{tr}\left(\mathbf{B}\mathbf{R}_s\mathbf{B}^H\right) + \sigma^2} \tag{15a}$$

$$\text{s.t.} \quad \gamma_k \geq \bar{\gamma}_k, \tag{15b}$$

$$\beta_{t,n}^2 + \beta_{r,n}^2 \leq 1, \forall n \in \mathcal{N}, \tag{15c}$$

$$\mathrm{tr}\left(\mathbf{W}\mathbf{W}^H + \mathbf{R}_r\right) \leq P_t, \tag{15d}$$

$$\mathbf{R}_r \succeq 0, \tag{15e}$$

where $\chi \triangleq \{\mathbf{W}, \mathbf{R}_s, \boldsymbol{\Theta}_r, \boldsymbol{\Theta}_t\}$ represents the optimization variables, $\beta_{t,n}^2 + \beta_{r,n}^2 \leq 1$ is the law of energy conservation as in (4), and P_s is the limitation of sum power for communication and radar perception.

B. Proposed FP-BCD Based Algorithm

In particular, we divide the set of optimal variables χ into two blocks, namely $\{\boldsymbol{\Theta}_r, \boldsymbol{\Theta}_t\}$ and $\{\mathbf{W}, \mathbf{R}_s\}$. Then, the BCD algorithm is invoked to solve each block iteratively while fixing the other one, which leads to the following two subproblems.

1) Subproblem With Respect to $\{\mathbf{W}, \mathbf{R}_s\}$: In the aforementioned preliminary problem (15a), the given formula is presented in a non-convex fractional form, which naturally lends itself to Dinkelbach's transformation within the realm of FP [14]. Such transformation is a effective technique capable of recasting fractional expressions into a linear computational format, the fractional term in the aforementioned problem, the subproblem with respect to $\{\mathbf{W}, \mathbf{R}_s\}$ can be reformulated as

$$\max_{\mathbf{W},\mathbf{R}_s} \quad \mathrm{tr}\left(\mathbf{A}\mathbf{R}_s\mathbf{A}^H\right) - y\left[\mathrm{tr}\left(\mathbf{B}\mathbf{R}_s\mathbf{B}^H\right) + \sigma^2\right] \tag{16a}$$

$$\text{s.t.} \quad \left(1 + \frac{1}{\gamma}\right)\mathbf{u}_k^H\mathbf{W}_k\mathbf{u}_k \geq \mathbf{u}_k^H\mathbf{R}_s\mathbf{u}_k + \sigma^2, \forall k \in \mathcal{K}, \tag{16b}$$

$$\mathrm{tr}\left(\mathbf{R}_s\right) \leq P_t, \tag{16c}$$

$$\mathbf{R}_s \succeq \sum_{k\in\mathcal{K}}\mathbf{W}_k, \tag{16d}$$

$$\mathbf{R}_r \succeq 0, \tag{16e}$$

$$\mathbf{W}_k \succeq 0, \forall k \in \mathcal{K}, \tag{16f}$$

where $\mathbf{u}_k^H = \mathbf{h}_k^H\boldsymbol{\Theta}_t\mathbf{G}_t$ denotes the effective channel vector for user k, y, σ^2 are considered as constant terms. Constraint (16b) is transformed from the communication SINR constraint (15b), and $\mathbf{W}_k = \mathbf{w}_k\mathbf{w}_k^H$. We initially focus on optimizing the variable y within the context of the objective function. Based on [14], the closed-form solution for y is derived as follow

$$y = \frac{\mathrm{tr}\left(\mathbf{A}\mathbf{R}_s\mathbf{A}^H\right)}{\mathrm{tr}\left(\mathbf{B}\mathbf{R}_s\mathbf{B}^H\right) + \sigma^2}. \tag{17}$$

To solve the problem (16), it is evident that the condition $\mathrm{rank}\left(\mathbf{W}_k\right) = 1$, pertaining to the rank of the matrix $\mathbf{w}_k$, which introduces a non-convex characteristic. Consequently, a relaxation technique becomes imperative to streamline the solution process and ultimately yield a solution satisfying prescribed rank constraint of the matrix $\mathbf{w}_k$, which inspires us to solve it with semidefinite relaxation (SDR) algorithm.

The relaxed formulation (16) constitutes a convex problem, enabling the efficient attainment of its global optimum through existing convex optimization solvers. However, it is noteworthy that the omission of the rank-one constraint in this relaxation may result in the global optimum of (16) having a higher rank, which may not make the solution of the relaxed problem the solution of the original non-convex problem (15). Fortunately, in the proposition that follows, we demonstrate that it can always construct the rank-one feasible solution of the original problem (15) from an arbitrary global optimum of the relaxed problem (16).

Given an arbitrary global optimum $\tilde{\mathbf{R}}_s$ and $\tilde{\mathbf{w}}_k$ of problem (16), the desired matrix rank-one properties can be achieved through the application of the formula $\mathbf{R}_s^* = \tilde{\mathbf{R}}_s$. Subsequently, the optimized precoding vector $\mathbf{w}_k^*$ is derived as

$$\mathbf{w}_k^* = \left(\mathbf{u}_k^H\tilde{\mathbf{w}}_k\mathbf{u}_k\right)^{-\frac{1}{2}}\tilde{\mathbf{w}}_k\mathbf{u}_k. \tag{18}$$

Furthermore, the modified signal covariance matrix $\mathbf{R}_r^*$ is obtained by subtracting the contribution of the optimized precoding vectors from $\mathbf{R}_r^*$:

$$\mathbf{R}_r^\star = \mathbf{R}_s^\star - \sum_{k\in\mathcal{K}}\mathbf{w}_k^\star\left(\mathbf{w}_k^\star\right)^H. \tag{19}$$

This formulation ensures that the resultant matrices satisfy the rank-1 constraint.

2) Subproblem With Respect to $\{\boldsymbol{\Theta}_r, \boldsymbol{\Theta}_t\}$: The subproblem with respect to $\{\boldsymbol{\Theta}_r, \boldsymbol{\Theta}_t\}$ is given by

$$\max_{\boldsymbol{\Theta}_r,\boldsymbol{\Theta}_t} \quad \frac{\mathrm{tr}\left(\mathbf{A}\mathbf{R}_s\mathbf{A}^H\right)}{\mathrm{tr}\left(\mathbf{G}_r\boldsymbol{\Theta}_r\mathbf{G}_t\mathbf{R}_s\mathbf{G}_t^H\boldsymbol{\Theta}_r^H\mathbf{G}_r^H\right)+\sigma^2} \tag{20a}$$

$$\text{s.t.} \quad \beta_{t,n}^2 + \beta_{r,n}^2 \le 1, 0 \le \beta_{t,n}, \beta_{r,n} \le 1, \quad \forall n \in \mathcal{N}, \tag{20b}$$

$$\gamma_k \ge \bar{\gamma}_k, \quad \forall k \in \mathcal{K}. \tag{20c}$$

Evidently, the initial problem formulation (20) can be directly reformulated as problem (21), given that $\mathrm{tr}\left(\mathbf{A}\mathbf{R}_s\mathbf{A}^H\right)$ remains unaffected by the variation in the set of variables $\{\boldsymbol{\Theta}_r, \boldsymbol{\Theta}_t\}$. Based on the above assumptions, we reduce the optimization objective function (20a) in the fractional form to the non-fractional form (21a), which is convenient for subsequent computational processing.

$$\min_{\boldsymbol{\Theta}_r,\boldsymbol{\Theta}_t} \quad \left[\mathrm{tr}\left(\mathbf{G}_r\boldsymbol{\Theta}_r\mathbf{G}_t\mathbf{R}_s\mathbf{G}_t^H\boldsymbol{\Theta}_r^H\mathbf{G}_r^H\right)+\sigma^2\right] \tag{21a}$$

$$\text{s.t.} \quad \beta_{t,n}^2 + \beta_{r,n}^2 \le 1, 0 \le \beta_{t,n}, \beta_{r,n} \le 1, \quad \forall n \in \mathcal{N}, \tag{21b}$$

$$\gamma_k \ge \bar{\gamma}_k, \quad \forall k \in \mathcal{K}. \tag{21c}$$

To facilitate the optimization of $\boldsymbol{\Theta}_r$ and $\boldsymbol{\Theta}_t$, we transform the objective function and the communication SINR constraint into more tractable forms, where we define $\tilde{\mathbf{R}_x} = \mathbf{G}_t\mathbf{R}_s\mathbf{G}_t^H$. Moreover, the decomposition of the eigenvalue of the matrix $\tilde{\mathbf{R}_x}$ is given by

$$\tilde{\mathbf{R}}_x = \sum_{j=1}^{R}\varrho_j\mathbf{v}_j\mathbf{v}_j^H = \sum_{j=1}^{R}\tilde{\mathbf{v}}_j\tilde{\mathbf{v}}_j^H, \tag{22}$$

where $\tilde{\mathbf{v}}_j = \sqrt{\varrho_j}\mathbf{v}_j$ with ϱ_j and $\mathbf{v}_j$ denoting the eigenvalue and the corresponding eigenvector, and R denotes the rank of the matrix $\tilde{\mathbf{R}_x}$. Therefore, the objective function can be reformulated as

$$\begin{aligned}&\mathrm{tr}\left(\sum_{j=1}^{R}\mathbf{G}_r\boldsymbol{\Theta}_r\tilde{\mathbf{v}}_j\tilde{\mathbf{v}}_j^H\boldsymbol{\Theta}_r^H\mathbf{G}_r^H\right)\\ =&\mathrm{tr}\left(\sum_{j=1}^{R}\mathbf{G}_r\mathrm{diag}\left(\tilde{\mathbf{v}}_j\right)\boldsymbol{\theta}_r\boldsymbol{\theta}_r^H\mathrm{diag}\left(\tilde{\mathbf{v}}_j^H\right)\mathbf{G}_r^H\right).\end{aligned} \tag{23a}$$

Next, we define $\mathbf{G}_r\mathrm{diag}\left(\tilde{\mathbf{v}}_j\right) = \mathbf{V}_j$. Accordingly, problem (20) can be rewritten as

$$\min_{\boldsymbol{\Theta}_r,\boldsymbol{\Theta}_t} \quad \mathrm{tr}\left(\sum_{j=1}^{R}\mathbf{V}_j\boldsymbol{\theta}_r\boldsymbol{\theta}_r^H\mathbf{V}_j^H\right) \tag{24a}$$

$$\text{s.t.} \quad \beta_{t,n}^2 + \beta_{r,n}^2 \le 1, 0 \le \beta_{t,n}, \beta_{r,n} \le 1, \quad \forall n, \tag{24b}$$

$$\gamma_k \ge \bar{\gamma}_k, \quad \forall k. \tag{24c}$$

Then, we define the following variables given by

$$\boldsymbol{\Phi}_{k,i} = \mathrm{diag}\left(\mathbf{h}_k^H\right)\mathbf{G}\mathbf{w}_i\mathbf{w}_i^H\mathbf{G}^H\mathrm{diag}\left(\mathbf{h}_k\right), \tag{25a}$$

$$\boldsymbol{\Psi}_k = \mathrm{diag}\left(\mathbf{h}_k^H\right)\mathbf{G}\mathbf{R}_r\mathbf{G}^H\mathrm{diag}\left(\mathbf{h}_k\right). \tag{25b}$$

As a consequence, problem (23) can be rewritten as

$$\min_{\boldsymbol{\Theta}_r,\boldsymbol{\Theta}_t} \quad \mathrm{tr}\left(\sum_{j=1}^{R}\mathbf{V}_j\boldsymbol{\theta}_r\boldsymbol{\theta}_r^H\mathbf{V}_j^H\right) \tag{26a}$$

$$\text{s.t.} \quad \frac{1}{\bar{\gamma}_k}\boldsymbol{\theta}_t^H\boldsymbol{\Phi}_{k,k}^*\boldsymbol{\theta}_t \ge \sum_{i\in\mathcal{K}\setminus k}\boldsymbol{\theta}_t^H\boldsymbol{\Phi}_{k,i}^*\boldsymbol{\theta}_t + \boldsymbol{\theta}_t^H\boldsymbol{\Psi}_k^*\boldsymbol{\theta}_t + \sigma^2, \quad \forall k, \tag{26b}$$

$$\left|\left[\boldsymbol{\theta}_t\right]_n\right|^2 + \left|\left[\boldsymbol{\theta}_r\right]_n\right|^2 \le 1, \quad \forall n. \tag{26c}$$

Upon observing that both the objective function and all constraints of problem (26) are quadratic in terms of the optimization variables, we leverage the SDR method to approximate its solution. Therefore, we introduce auxiliary variables $\mathbf{Q}_i = \boldsymbol{\theta}_i\boldsymbol{\theta}_i^H$ for all $i \in \{t, r\}$, which are subject to the

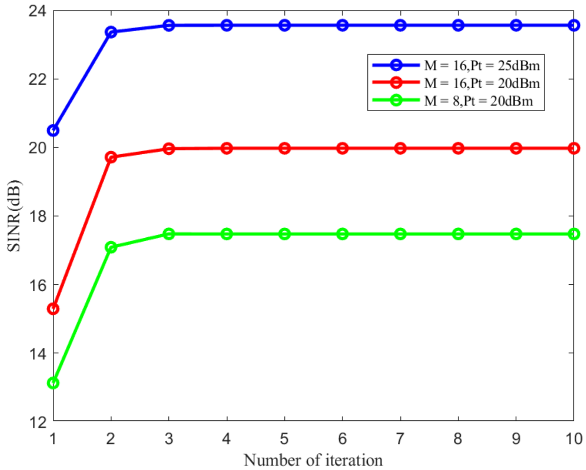

Fig. 2. The covergence behavior of proposed FP-BCD based algorhithm.

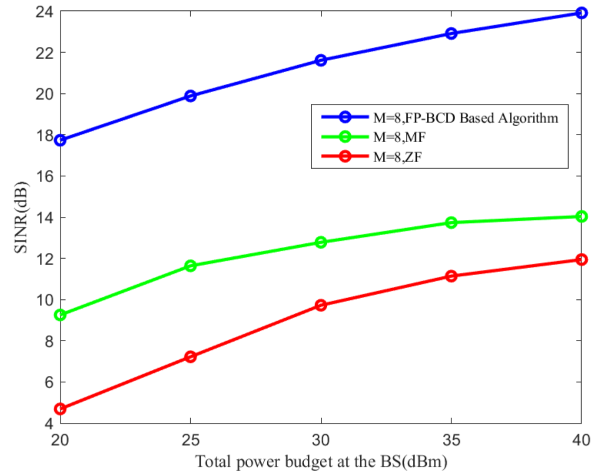

Fig. 3. Radar SINR versus total power budget P_t for $M = 8$.

conditions $\mathbf{Q}_i \succeq 0$ and $\mathrm{rank}(\mathbf{Q}_i) = 1$. Subsequently, the SDR reformulation of problem (26) can be mathematically expressed as

$$\min_{\boldsymbol{\Theta}_r, \boldsymbol{\Theta}_t} \quad \mathrm{tr}\left(\sum_{j=1}^{R} \mathbf{V}_j \mathbf{Q}_r \mathbf{V}_j^H\right) \tag{27a}$$

$$\text{s.t.} \quad \frac{1}{\gamma_k}\mathrm{tr}\left(\boldsymbol{\Phi}_{k,k}^* \mathbf{Q}_t\right) \geq \sum_{i \in \mathcal{K}\setminus k} \mathrm{tr}\left(\boldsymbol{\Phi}_{k,i}^* \mathbf{Q}_t\right), \tag{27b}$$

$$+ \mathrm{tr}\left(\boldsymbol{\Psi}_k^* \mathbf{Q}_t\right) + \sigma_k^2, \quad \forall k, \tag{27c}$$

$$[\mathbf{Q}_t]_{n,n} + [\mathbf{Q}_r]_{n,n} \leq 1, \quad \forall n, \tag{27d}$$

$$\mathbf{Q}_t \succeq 0, \quad \mathbf{Q}_r \succeq 0. \tag{27e}$$

The problem (27) can be further identified as a convex SDR, thus enabling the efficient attainment of its global optimum through the utilization of existing convex optimization solvers. Notably, although the SDR may yield a solution with a general rank, techniques such as eigenvalue decomposition can be invoked to devise a feasible rank-one solution for problem (23).

The algorithm initializes with a random variable denoted as χ. Then, it enters a loop to iteratively update two sets of variables: $\{\mathbf{W}, \mathbf{R}_s\}$ and $\{\boldsymbol{\Theta}_r, \boldsymbol{\Theta}_t\}$. 1) Updating $\{\mathbf{W}, \mathbf{R}_s\}$: The inner update involves calculating an intermediate variable y and then using this y to determine the new values of $\{\mathbf{W}, \mathbf{R}_s\}$. The inner loop continues until the convergence criterion $| \gamma_r - \gamma_{r-pre} | \leq \varepsilon$ is met, where γ_r and γ_{r-pre} represent the objective values at the current and previous iterations, respectively, and ε is a predefined tolerance level.

2) Updating $\{\boldsymbol{\Theta}_r, \boldsymbol{\Theta}_t\}$: The outer loop continues these alternating updates until the overall convergence criterion $| \gamma_r - \gamma_{r-pre} | \leq \varepsilon$ is satisfied, indicating that the algorithm has converged to a solution within the specified tolerance.

The computational complexity of the proposed algorithm is primarily determined by the complexities of solving problem (16) and problem (27). Assuming the solution accuracy is ϵ, the complexities of solving problem (16) and problem (27) are $\mathcal{O}((K^{6.5}M^{6.5}+N^{6.5})\log(\frac{1}{\epsilon}))$ and $\mathcal{O}((K+N)^{6.5}N^{6.5}\log(\frac{1}{\epsilon}))$, respectively.

IV. Numerical Results

In this section, simulation results are presented to verify the convergence and effectiveness of the proposed algorithm. Considering a three-dimensional Cartesian coordinates system, we assume that STAR-RIS is located at the origin. Therefore, the coordinates of STAR-RIS are $(0m, 0m, 0m)$. The location of the base station is assumed to be at $(25\sqrt{3}m, 25m, 0m)$, and the location of the target is assumed to be at $(0m, 50m, 0m)$. Based on geometric reasoning, the distance between the BS and the target is 50 meters, and the azimuth DOA of the target relative to the BS is 30°. Assuming the path loss is

$$p = c_0(d)^{-\alpha_d}, \tag{28}$$

where $c_0 = -30$ dB, $\alpha_d = 2.2$ and d represents the distance relative to STAR-RIS. All channels are assumed to follow Rician fading with a Rician factor of 3 dB. The spacing between antennas is half of the carrier wavelength λ. We assume that there are $K = 4$ users randomly distributed within $20 \sim 50$ m from the STAR-RIS in communication area. The required SINR threshold for each user is 20 dB, i.e., $\gamma = 20$ dB. Without loss of generality, we set noise power $\sigma^2 = -110$ dBm, convergence threshold $\varepsilon = 10^{-3}$.

A. Convergence Performance of the Proposed Algorithms

In Fig.2, we assess the convergence performance of the proposed algorithm in the context of a random channel implementation. Notably, the initialization point for the algorithm is chosen randomly. It can be observed that the proposed algorithm demonstrates robust convergence within 5 iterations. Furthermore, When other conditions remain unchanged, both the increase in the number of antennas and the enhancement of the maximum power constraint can lead to improved radar SINR.

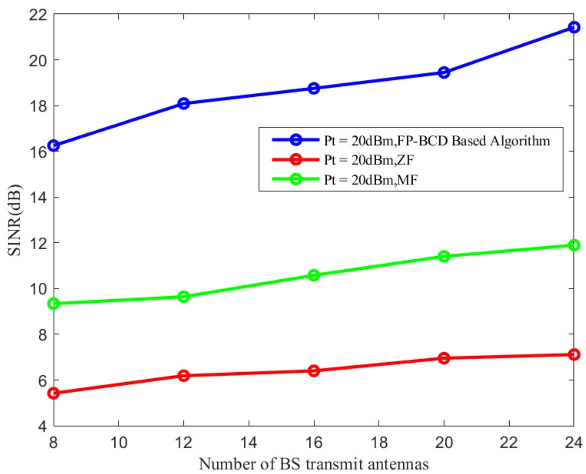

Fig. 4. Radar SINR versus Number of STAR-RIS elements M for $P_t = 20dBm$.

B. Radar SINR versus Total Power Budget

In Fig.3, we investigate the impact of the total transmit power constraint P_t on the performance of the FP-BCD based algorithm, where zero-forcing (ZF) and matching filtering (MF) algorithms are selected for comparison. The number of transmit antennas at the BS is set to $M = 8$. It can be observed from the figure that as P_t increases, the radar SINR of all three algorithms increase accordingly, and the proposed algorithm exhibits significant performance improvements compared to the ZF algorithm and the MF algorithm. The aforementioned phenomenon demonstrates the effectiveness of the FP-BCD based algorithm.

C. Radar SINR versus Number of STAR-RIS elements

In Fig.4, we study the impact of the number of transmit antennas M on FP-BCD based algorithm performance under a fixed constraint of maximum transmit power $P_t = 20$ dBm. It is observed that as M increases, the radar SINR obtained by all three algorithms monotonically increases. Compared to the ZF and MF algorithms, the FP-BCD Based Algorithm exhibits significantly superior performance, thereby demonstrating its effectiveness.

V. Conclusion

In this paper, we investigated an ISAC system assisted by STAR-RIS. We formulate an optimization problem for maxmizing radar SINR based on constraints of communication SINR, maximum transmit power limitation, and the law of conservation of energy. To address this problem, we propose a novel algorithm based on FP and BCD, and employ SDR to solve the problem. Based on our proposed algorithm, we can optimize beamforming matrix as well as the reflection and transmission phase shift matrices. Simulation results demonstrate that the proposed algorithm exhibits good convergence properties and significant performance improvements compared to the state-of-the-art algorithms.

Ackonwledgements

This work was supported in part by the National Key Research and Development Program of China under Grant2024YFE0200404. H. Hou was supported by the National Natural Science Foundation of China under Grant No. 62203109, the Natural Science Foundation of Jiangsu Province under Grant No. BK20220812, and China Postdoctoral Science Foundation No. 2023M742671.

References

[1] H. Tataria, M. Shafi, A. F. Molisch, M. Dohler, H. Sjöland and F. Tufvesson, ”6G wireless systems: Vision, requirements, challenges, insights, and opportunities,” *Proc. IEEE*, vol. 109, no. 7, pp. 1166-1199, Jul. 2021.

[2] H. Luo, R. Liu, M. Li and Q. Liu, ”RIS-aided integrated sensing and communication: Joint beamforming and reflection design,” *IEEE Trans. Veh. Technol.*, vol. 72, no. 7, pp. 9626-9630, Jul. 2023.

[3] A. Papazafeiropoulos, P. Kourtessis and S. Chatzinotas, ”STAR-RIS-assisted communication radar coexistence: Analysis and optimization,” *IEEE Trans. Veh. Technol.*, vol. 73, no. 9, pp. 13381-13395, Sep. 2024.

[4] F. Liu, C. Masouros, A. P. Petropulu, H. Griffiths, and L. Hanzo, “Joint radar and communication design: Applications, state-of-the-art, and the road ahead,” *IEEE Trans. Commun.*, vol. 68, no. 6, pp. 3834–3862, Jun. 2020.

[5] F. Liu, L. Zhou, C. Masouros, A. Li, W. Luo, and A. Petropulu, “Toward dual-functional radar-communication systems: Optimal waveform design,” *IEEE Trans. Signal Process.*, vol. 66, no. 16, pp. 4264–4279, Aug. 2018.

[6] L. Zheng, M. Lops, Y. C. Eldar, and X. Wang, “Radar and communication coexistence: An overview: A review of recent methods,” *IEEE Signal Process. Mag.*, vol. 36, no. 5, pp. 85–99, Sep. 2019.

[7] M. Labib, V. Marojevic, A. F. Martone, J. H. Reed, and A. I. Zaghloui, “Coexistence between communications and radar systems: A survey,” URSI Radio Sci. Bull., vol. 2017, no. 362, pp. 74–82, Sep. 2017.

[8] Z. Wang, X. Mu and Y. Liu, ”STAR-RIS enabled integrated sensing and communications,” *IEEE Trans. Wireless Commun.* , vol. 22, no. 10, pp. 6750-6765, Oct. 2023.

[9] Z. Liu, X. Li, H. Ji, H. Zhang and V. C. M. Leung, ”Toward STAR-RIS-empowered integrated sensing and communications: Joint active and passive beamforming design,” *IEEE Trans. Veh. Technol*, vol. 72, no. 12, pp. 15991-16005, Dec. 2023.

[10] Z. Yu *et al.*, ”Active RIS-aided ISAC systems: Beamforming design and performance analysis,” *IEEE Trans. Commun.*, vol. 72, no. 3, pp. 1578-1595, Mar. 2024.

[11] Z. Yu, X. Hu, C. Liu, M. Peng and C. Zhong, ”Location sensing and beamforming design for IRS-enabled multi-user ISAC systems,” *IEEE Trans. Signal Process.*, vol. 70, pp. 5178-5193, 2022.

[12] K. Chen, C. Qi, O. A. Dobre and G. Y. Li, ”Simultaneous beam training and target sensing in ISAC systems with RIS,” *IEEE Trans. Wireless Commun.*, vol. 23, no. 4, pp. 2696-2710, Apr. 2024.

[13] M. Hua, Q. Wu, C. He, S. Ma and W. Chen, ”Joint active and passive beamforming design for IRS-aided radar-communication,” *IEEE Trans. Wireless Commun.*, vol. 22, no. 4, pp. 2278-2294, Apr. 2023.

[14] K. Shen and W. Yu, ”Fractional programming for communication systems—Part I: Power control and beamforming,” *IEEE Trans. Signal Process.*, vol. 66, no. 10, pp. 2616-2630, May 2018.

[15] Y. He, Y. Cai, H. Mao and G. Yu, ”RIS-assisted communication radar coexistence: Joint beamforming design and analysis,” *IEEE J. Sel. Areas Commun.*, vol. 40, no. 7, pp. 2131-2145, Jul. 2022.

[16] Y. Cui, F. Liu, X. Jing and J. Mu, ”Integrating sensing and communications for Ubiquitous IoT: Applications, trends, and challenges,” *IEEE Network*, vol. 35, no. 5, pp. 158-167, Sep. 2021.

[17] L. Lu, G. Y. Li, A. L. Swindlehurst, A. Ashikhmin and R. Zhang, ”An overview of massive MIMO: Benefits and challenges,” *IEEE J. Sel. Topics Signal Process.*, vol. 8, no. 5, pp. 742-758, Oct. 2014.

[18] X. Su et al., ”Reconfigurable intelligent surfaces: Standardization oriented analysis and considerations,” *IEEE Commun. Stand. Mag.*, vol. 8, no. 4, pp. 40-46, December 2024.